

# Strong Fundamental Rejection in Frequency Doublers at 220-260 GHz Using a 250-nm InP HBT Process

Jeff Shih-Chieh Chien<sup>#,\*</sup>, Ethan Lam<sup>#</sup>, Jonathan Tao<sup>#</sup>, James F. Buckwalter<sup>#</sup>

<sup>#</sup>Department of Electrical and Computer Engineering, University of California, Santa Barbara, USA

<sup>\*</sup>Samsung Semiconductor, Inc., San Jose, USA

**Abstract**— Two frequency doublers operating at 220-260 GHz offer high fundamental rejection in a 250-nm Indium Phosphide (InP) HBT process. A second-harmonic termination technique at the input is adopted in both designs to improve collector efficiency ( $\eta$ ) and fundamental rejection. The first of the two designs achieves 6.8-dBm peak output power at 220-260 GHz with -3.3 dB peak conversion gain, 17.7% peak  $\eta$  and more than 29.3 dB fundamental rejection. The second design adopting a novel tunable notch filter for fundamental rejection improvement achieves 1.2-dBm peak output power at 220-260 GHz with -14.4 dB peak conversion gain, 6.7% peak  $\eta$  and >54.7 dB fundamental rejection. To our knowledge, these frequency multipliers demonstrate improved harmonic rejection.

**Keywords**— millimeter wave, G-band, frequency doubler, frequency multiplier, InP HBT

## I. INTRODUCTION

Upper millimeter-wave (mm-wave) bands ranging from 110 GHz to 300 GHz have gained more attention for next generation sensing and beyond-5G communication systems in recent years [1][2] due to the high resolution for imaging and larger channel bandwidth for high data rate applications [3]. G-band (140-220 GHz) is one of the most discussed band due to reasonable circuit performance from current available technology such as SiGe HBT, InP HBT or InP pHEMT.

In a sensing system, frequency-modulated continuous-wave (FMCW) radar is commonly adopted at upper mm-wave bands to leverage available wide-band channels to achieve high spatial resolution [4]. Multipliers that include frequency doublers or triplers are designed to enable low frequency local oscillator or chirp synthesizer. These multipliers are required to suppress the fundamental component of the FMCW signal to eliminate a leakage tone at the output that will interfere with any out-of-band signals on the transmitter and avoid folding noise or unwanted signal into band of interest on receiver. Similarly in a communication systems, the multiplier is required to provide high fundamental rejection to prevent EVM degradation on both transmitter and receiver.

Several recent publications have shown promising performance of push-push frequency doublers from 110 GHz to 300 GHz. The transmission line based input reflector is added on push-push frequency doubler for improving output power and  $\eta$  [5][6]. Gm-boosted push-push frequency doubler is proposed in [7] for higher conversion gain as well as better  $\eta$ . However, previous research has not shown fundamental rejection of the input signal better than 30 dB.

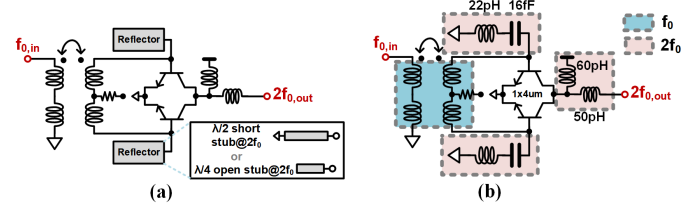


Fig. 1. Schematic of frequency doubler (a) with conventional input open or short stub reflector (b) input notch termination to isolate the  $2f_0$  component.

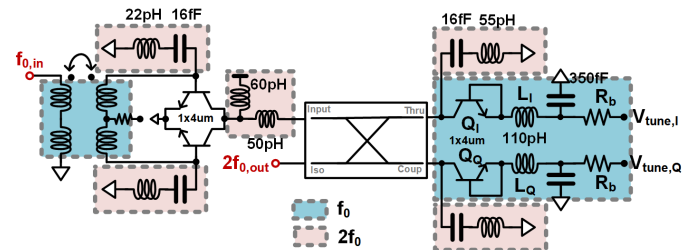


Fig. 2. Schematic of the proposed frequency doubler with input notch termination and novel reflective type tunable fundamental notch filter.

This paper presents architectures for the frequency doubler, realized in a 250-nm InP HBT process, that are capable of high output power, high  $\eta$ , and excellent fundamental output rejection. Section II describes the frequency doubler design and Section III will present measurement results.

## II. FREQUENCY DOUBLER DESIGN

### A. Push-push frequency doubler with input notch termination

Fig. 1(a) shows the conventional input reflector design proposed in [5][6]. Short stub design provides low impedance at  $2f_0$  while maintaining high impedance at  $f_0$ . Open stub design keeps low impedance at  $2f_0$  while presenting 45° open stub transmission line at  $f_0$ . Both open and short stub require area for transmission line and the spacing to other passive structures and therefore occupy substantial area. Fig. 1(b) shows the first proposed push-push frequency doubler with input balun, two notch filters and output matching network for obtaining highest  $2^{nd}$  harmonic output power. Two input notch filters work as capacitive loading on the input fundamental balun for compensating phase error between balanced port. With this degree of freedom, the loss and area of balun could be minimized for higher conversion gain. The notch filters also provide low impedance paths for  $2^{nd}$  harmonic feedback

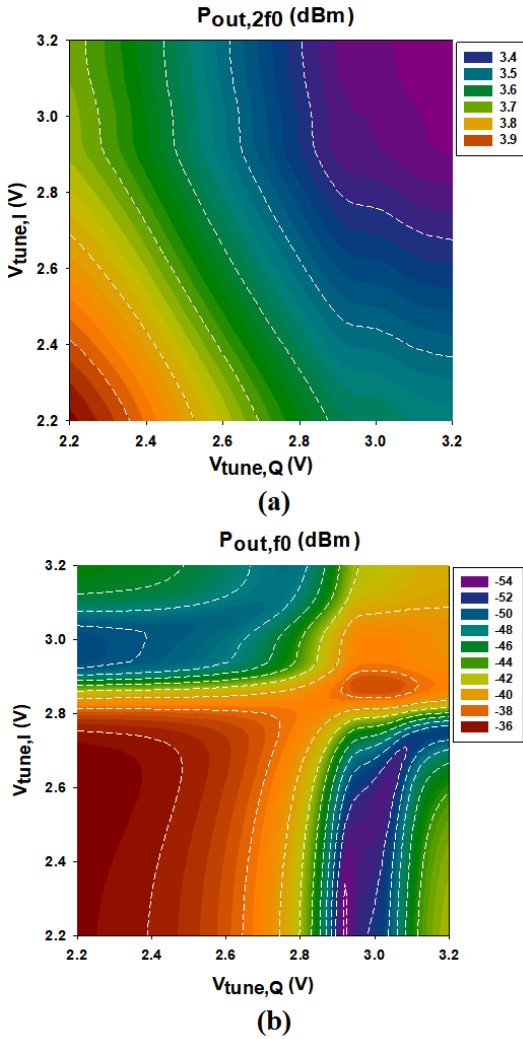


Fig. 3. (a) Output power at  $2f_0$  (b)output power at  $f_0$  with sweep of  $V_{tune,I}$  and  $V_{tune,Q}$ .

current through  $C_{bc}$ . This eliminates the negative feedback path that will lower the output power or  $\eta$ .

#### B. Tunable high-rejection fundamental notch filter

In [8], the concept of reflective signal addition and cancellation through independent loading on THRU and COUPLED ports of  $90^\circ$  hybrid coupler is introduced as ON or OFF state switch. To extend the concept to a tunable notch filter for high fundamental rejection frequency doubler, the impedance loading on the THRU and COUPLED ports of the  $90^\circ$  hybrid coupler satisfy an OFF-state switch condition at  $f_0$  ( $|\Gamma_{I,f_0}| = |\Gamma_{Q,f_0}|$ ,  $\angle\Gamma_{I,f_0} = \angle\Gamma_{Q,f_0} \pm \pi$ ) and ON-state switch condition at  $2f_0$  ( $\Gamma_{I,2f_0} = \Gamma_{Q,2f_0}$ ). As shown in Fig. 2, the second frequency doubler is formed using the original frequency doubler in Fig. 1(b) with a wide-band  $90^\circ$  hybrid coupler and two identical tunable loads. These two loads present C-L-C resonant loads at  $f_0$  that ensures an out-of-phase reflective signal from THRU and COUPLED ports. The varactors are implemented using the diode-connected HBT

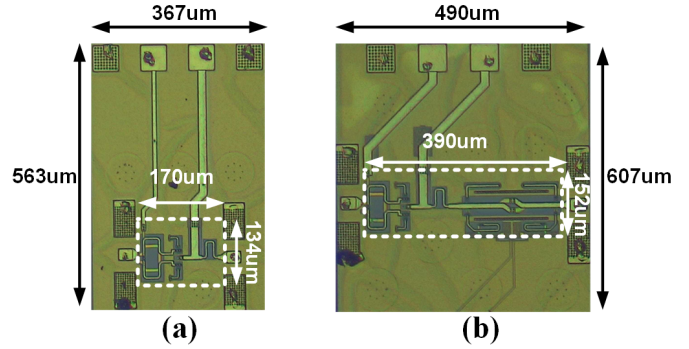


Fig. 4. Chip photograph of the proposed push-push frequency doubler (a) without tunable notch filter (b) with tunable notch filter.

base-collector junction for larger  $C_{max}/C_{min}$  ratio and quality factor. At the  $2f_0$ , these two loads present identical high  $\Gamma$  reflection so insertion loss is minimized and determined by the loss of  $90^\circ$  hybrid coupler and  $\Gamma$  of these two loads at  $2f_0$ .

Simulated results of output power at  $2f_0$  and  $f_0$  with regard to the two independent tuning loads is shown in Fig. 3. With 8-dBm input power at 110 GHz, Fig. 3(a) shows the variation in the power at  $2f_0$  is less than 0.6 dB with the sweep of  $V_{tune,I}$  and  $V_{tune,Q}$  shown in Fig. 2. In Fig. 3(b), the output power at  $f_0$  ranges from -35 dBm to -54 dBm. The highest fundamental rejection bias could be determined by this plot with  $V_{tune,I} = 2.22$  V and  $V_{tune,Q} = 2.92$  V. All the frequency points are optimized in the same flow and therefore this topology is feasible for achieving wideband strong fundamental rejection.

### III. MEASUREMENT RESULTS

Two frequency doublers are implemented in 250-nm InP HBT process and the chip photograph is shown in Fig. 4. The core area for two designs are  $0.023\text{mm}^2$  and  $0.059\text{mm}^2$ .

Large signal measurements for the second harmonic were done using a D-band input source consisting of a WR6.5 frequency extender driven from the N5247A PNA-X. The extenders drive a narrow-band VDI D-band power amplifier with input power control through the 511D Mi-Wave electronically tunable attenuator. An output isolator is placed after the power amplifier to prevent reflections back into the amplifier. The input is probed with WR6 probes from GGB, with a measured loss of about 1.85 dB at D-band. The output is probed using WR4 probes from GGB with about 3dB of insertion loss. The second harmonic power is detected using the WR4.3SHM subharmonic mixer and the N9030B spectrum analyzer. The LO is driven using a VDI WR6.5 frequency extender driven by an external frequency source at 9.98 GHz. Attenuators are placed at the RF and LO to prevent damage to the mixer. The input and output were calibrated using the PM5B power meter and WR4.3-SGX. Fundamental rejection measurements were done using the same input setup, but the output is replaced and calibrated with the output frequency extender into the PNAX. Both measurement setups are shown on Fig. 5.

Table 1. Performance Comparison of 170-260 GHz Frequency Doublers

	Frequency (GHz)	Technology	Topology	Peak Pout (dBm)	Peak Conversion Gain (dB)	Peak $\eta$ (%)	Fundamental Rejection (dB)
<b>This Work</b>	<b>220-260</b>	<b>250-nm InP HBT</b>	<b>Push-push with input notch termination</b>	<b>6.8</b>	<b>-3.3</b>	<b>17.7</b>	<b>29.3-45.3</b>
<b>This Work</b>	<b>220-260</b>	<b>250-nm InP HBT</b>	<b>Push-push with input notch termination + reflective type tunable notch filter</b>	<b>1.2</b>	<b>-14.4</b>	<b>6.7</b>	<b>54.7-73.9</b>
[5]	200-245	90-nm SiGe	Push-push with input short-stub reflectors	2	-15	4.5	15-25
[9]	208-233	28-nm CMOS	Neutralized driver+push-push	-4.9	-7.2	1.1	-
[10]	222-250	90-nm SiGe	Push-push	1.8	-15	1.7	>30
[10]	200-230	90-nm SiGe	4-stage driver+push-push+4-way power combiner	8	1.6	0.2	>25
[6]	160-220	130-nm SiGe	Push-push with input open-stub reflector	-2.6	-8.6	1.4	-
[6]	170-230	130-nm SiGe	2-way PA+push-push with input open-stub reflector	6.5	4.5	1.1	-
[11]	140-220	800-nm InP HBT	Push-push	8.2	-8.8	16.1	-
[7]	190-205	800-nm InP HBT	Gm boosted push-push	4.7	-5.3	9.6	17.5
[7]	170-200	800-nm InP HBT	Gm boosted push-push + cascode	5.4	-5.6	6.1	17.3
[12]	160-310	65-nm CMOS	Pre-amplifier with push-push	3	3	2.8	>40
[13]	235-265	65-nm CMOS	Embedded network with input open-stub reflector	0.9	-4	2.9	17-25

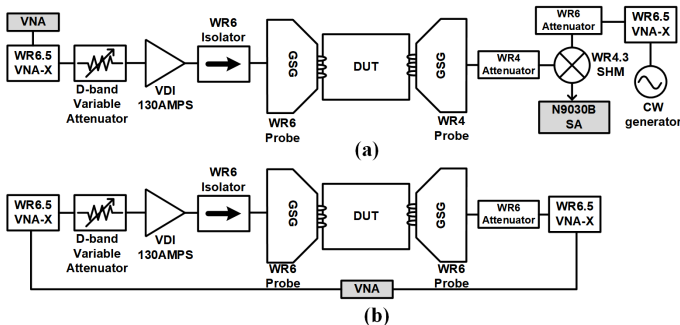


Fig. 5. (a) Power measurement setup for output frequency of 220-260 GHz  
(b) power measurement setup for output frequency of 110-130 GHz.

Second harmonic output power was measured from 220 to 260 GHz in 4 GHz steps with swept power from the electronic attenuator. Fig. 6 and Fig. 7 shows measured output power at  $f_0$  and  $2f_0$ ,  $\eta$  and conversion gain with input power sweep at 110-GHz for both designs. Measured performance of two frequency doublers across frequency are shown in Fig. 8 and Fig. 9. Measurements of the doubler without the notch indicate a maximum output power of 6.8 dBm at 224 GHz with associated  $\eta$  of 14.2% and conversion gain of -8.7 dB.  $\eta$  above 10% is achieved from about 222 GHz to 257 GHz. Including the notch, the measured peak output power was 1.2 dBm at 224 GHz with associated  $\eta$  of 6.3% and conversion gain of -15.3 dB.

At 224 GHz, the fundamental rejection is 29.3 dB without the notch and better than 54.7 dB with the tunable notch. Bias voltages for the tunable notch were adjusted over frequency to attain best possible fundamental rejection at 220 to 250 GHz at 10 GHz steps. With the tunable notch, the fundamental rejection is improved by over 30 dB across frequency, however output power decreases by about 5-12 dB. Consequently, the  $\eta$  drops significantly. Table 1 summarizes the state-of-the-art 170-260 GHz frequency doublers for the comparison of the presented work.

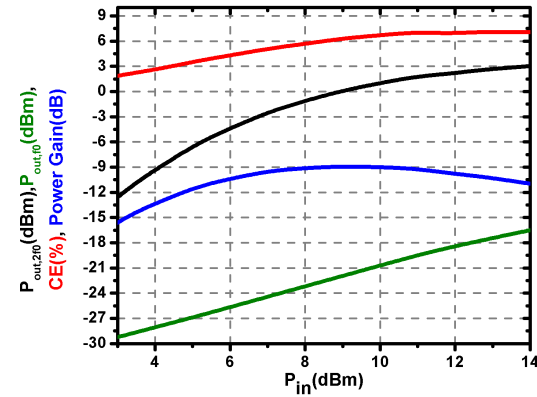


Fig. 6. Measured output power at  $f_0$  and  $2f_0$ ,  $\eta$  and conversion gain with input power sweep at 110 GHz for frequency doubler without tunable notch filter.

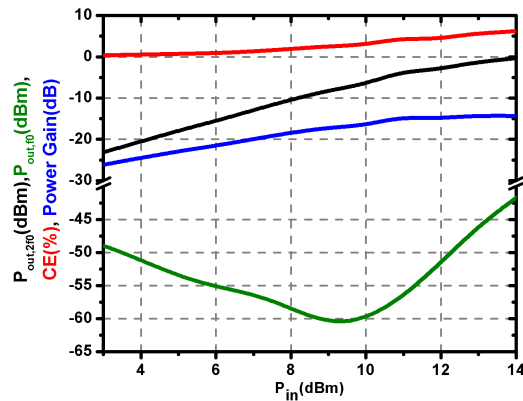


Fig. 7. Measured output power at  $f_0$  and  $2f_0$ ,  $\eta$  and conversion gain with input power sweep at 110 GHz for frequency doubler with tunable notch filter.

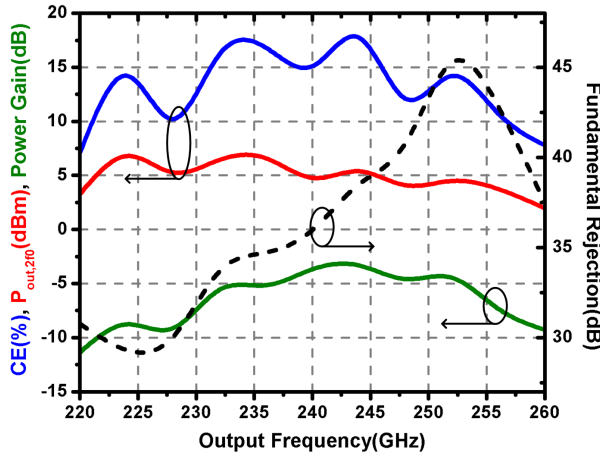


Fig. 8. Measured output power at  $2f_0$ ,  $\eta$ , conversion gain and fundamental rejection with input power sweep at 110 GHz for frequency doubler without notch filter.

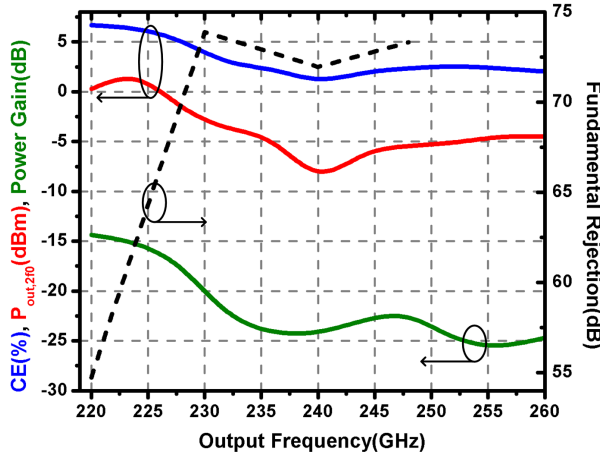


Fig. 9. Measured output power at  $2f_0$ ,  $\eta$ , conversion gain and fundamental rejection with input power sweep at 110 GHz for frequency doubler with notch filter.

#### IV. CONCLUSION

We demonstrate two frequency doublers operating at 220–260 GHz output frequency with high fundamental rejection. Both designs contain an input-notch terminated push-push topology. However, we propose the use of a novel reflective tunable notch filter that shows strong fundamental rejection. The two designs show peak output power of 6.8-dBm and 1.2-dBm, peak  $\eta$  of 17.7% and 6.7% while maintaining fundamental rejection better than 29.3 dB and 54.7 dB, respectively.

#### ACKNOWLEDGMENT

This work was supported by the Semiconductor Research Corporation (SRC) and DARPA under the JUMP program (ComSenTer). The authors would like to thank Teledyne Scientific and Imaging for the IC fabrication.

#### REFERENCES

- [1] J. C. Balzer, C. J. Saraceno, M. Koch, P. Kaurav, U. R. Pfeiffer, W. Withayachumnankul, T. Kürner, A. Stöhr, M. El-Absi, A. A.-H. Abbas, T. Kaiser, and A. Czyliwki, "THz Systems Exploiting Photonics and Communications Technologies," *IEEE Journal of Microwaves*, vol. 3, no. 1, pp. 268–288, 2023.
- [2] M. J. W. Rodwell, A. A. Farid, A. S. H. Ahmed, M. Seo, U. Soylu, A. Alizadeh, and N. Hosseiniyeh, "100-300GHz Wireless: ICs, Arrays, and Systems," in *2021 IEEE BiCMOS and Compound Semiconductor Integrated Circuits and Technology Symposium (BCICTS)*, 2021, pp. 1–4.
- [3] P. Rodriguez-Vazquez, J. Grzyb, B. Heinemann, and U. R. Pfeiffer, "A QPSK 110-Gb/s Polarization-Diversity MIMO Wireless Link With a 220–255 GHz Tunable LO in a SiGe HBT Technology," *IEEE Transactions on Microwave Theory and Techniques*, vol. 68, no. 9, pp. 3834–3851, 2020.
- [4] K. B. Cooper, R. J. Dengler, N. Llombart, B. Thomas, G. Chattopadhyay, and P. H. Siegel, "Thz imaging radar for standoff personnel screening," *IEEE Transactions on Terahertz Science and Technology*, vol. 1, no. 1, pp. 169–182, 2011.
- [5] H.-C. Lin and G. M. Rebeiz, "A 200–245 GHz Balanced Frequency Doubler with Peak Output Power of +2 dBm," in *2013 IEEE Compound Semiconductor Integrated Circuit Symposium (CSICS)*, 2013, pp. 1–4.
- [6] K. Wu, S. Muralidharan, and M. M. Hella, "A Wideband SiGe BiCMOS Frequency Doubler With 6.5-dBm Peak Output Power for Millimeter-Wave Signal Sources," *IEEE Transactions on Microwave Theory and Techniques*, vol. 66, no. 1, pp. 187–200, 2018.
- [7] T. K. Johansen, A.-S. Thualfiqar, N. Weimann, W. Heinrich, and V. Krozer, "Balanced G-band Gm-boosted frequency doublers in transferred substrate InP HBT technology," in *2016 11th European Microwave Integrated Circuits Conference (EuMIC)*, 2016, pp. 89–92.
- [8] J. S.-C. Chien and J. F. Buckwalter, "Low Insertion Loss, Reflective-Load Switches Operating in D-Band and G-Band," *IEEE Transactions on Microwave Theory and Techniques*, vol. 71, no. 1, pp. 230–239, 2023.
- [9] H. Fu, K. Li, and K. Ma, "A 208–233-GHz Frequency Doubler With 1.1% Power-Added Efficiency in 28-nm CMOS," *IEEE Microwave and Wireless Components Letters*, vol. 32, no. 11, pp. 1311–1314, 2022.
- [10] H.-C. Lin and G. M. Rebeiz, "A SiGe Multiplier Array With Output Power of 5–8 dBm at 200–230 GHz," *IEEE Transactions on Microwave Theory and Techniques*, vol. 64, no. 7, pp. 2050–2058, 2016.
- [11] M. Hossain, K. Nosaeva, B. Janke, N. Weimann, V. Krozer, and W. Heinrich, "A G-Band High Power Frequency Doubler in Transferred-Substrate InP HBT Technology," *IEEE Microwave and Wireless Components Letters*, vol. 26, no. 1, pp. 49–51, 2016.
- [12] N. Sharma, W. Choi, and K. O. Kenneth, "160–310 GHz frequency doubler in 65-nm CMOS with 3-dBm peak output power for rotational spectroscopy," in *2016 IEEE Radio Frequency Integrated Circuits Symposium (RFIC)*, 2016, pp. 186–189.
- [13] B.-T. Moon, B. Yun, J. Kim, and S.-G. Lee, "Analysis and Design of Power-Efficient H-Band CMOS Frequency Doubler Employing Gain Boosting and Harmonic Enhancing Techniques," *IEEE Access*, vol. 11, pp. 34 942–34 951, 2023.